KIKS Extended Team Description for RoboCup 2026

Takahiro Miyauchi, Yota Dori, Chihiro Takanashi, Mizuki Nonoyama, Chiaki Naito, Masato Kato, Ryota Tsutsui, Isami Hayashi, Rukito Ban, Takashi Matsubara, Dai Oikawa, and Toko Sugiura

National Institute of Technology (KOSEN), Toyota College,
2-1 Eisei-cho, Toyota, Aichi 471-8525, Japan
sugiura.toko@toyota.kosen-ac.jp,
URL: https://www.ee.toyota-ct.ac.jp/staff/sugi/RoboCup.html

Abstract. In this paper, we present the development activities related to RoboCup pursued by KIKS team during 2025 to qualify for RoboCup 2026 in Incheon. In particular, we focused on the improvement and evaluation of a dribbling damper manufactured using 3D printers, and also regarding the goal-scoring ability of teams analyzed last year, we examined the chance of each team scoring during matches without restrictions on shooting situations by applying the OBSO model. Furthermore, we introduce the development of ultra-compact soccer robots specialized for educational purposes.

Keywords: RoboCup, small size league, autonomous robot, global vision, engineering education

1 Introduction

In 2025, we performed improvements and evaluations on the dribble damper manufactured with a 3D printer. Also, regarding the competitive performance (Expected Goals described in §3) of the RoboCup World Championship team analyzed last year, this time we examined the relationship between ball possession beyond shooting scenes and scoring ability. Additionally, we introduce the development of ultra-compact soccer robots specifically designed for educational purposes. The details of research and experiments are described in each section.

2 Damper Fabrication Using 3D Printers

In this chapter, we evaluated the ball-holding performance of the dribbler in front of the robot based on the shape and hardness of the dampers manufactured by 3D printer.

2.1 Fabrication of new damper units

The dribbling unit currently equipped on our robot is shown in Fig. 1. A thermoplastic elastomer shock-absorbing material is used as a damper, attached with double-sided tape to the elliptical area at the rear of the dribble unit (a circle shown in Fig. 1). This damper, however, often detaches during matches, affecting the chip kick mechanism. Thus, in this chapter, we manufactured a new dribbling unit by referencing the damper structure of the dribbler unit of the 2024 champion team TIGERs[1], shown in Fig. 2. The Dribbler of the TIGERs team has dampers fitted in three locations. The Top Damper is primarily used to absorb the impact energy of the pass. The Slider plays a role in releasing the force of the backspin impact on the ball—that is, the force pushing the entire dribbler upward—while the ball is properly controlled. The small Bottom Damper is designed to attenuate the vertical vibrations of the dribbler caused by minor collisions with opponent robots and the roughness of the field surface during dribbling. Although the number and positions of dampers may vary, all teams have implemented similar damper mechanisms. This chapter focuses on evaluating the Slider and Top Damper, which are particularly effective at absorbing ball impact (Fig.3).

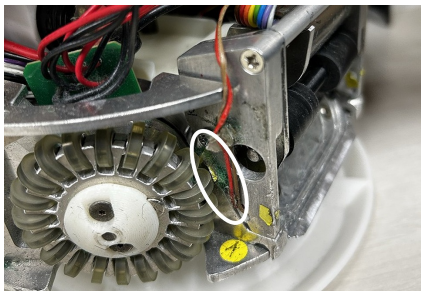

Fig. 1. A present damper used on our robot.

2.2 Evaluation of various damper performance

In this experiment, two types of materials were used for the Top Damper: a softer black sponge made of natural rubber (NR) (10 mm thick) and a harder gray sponge made of polyethylene (5 mm thick), as shown in Fig. 4. On the other hand, for the Slider material, we prepared six different dampers, as shown in Fig.5, 3D-printed from two types of flexible filament with three patterns of internal shape. We used KEYENCE AR-G1H silicone rubber-like filament (Shore A65)[2] and FlashForge TPU-F142 (Thermoplastic Polyurethane resin, Shore 95A) for the 3D filaments[3]. ①-③ were made from softer silicone rubber-like material, while ④-⑥ were made from harder TPU. ① and ④, ② and ⑤, and

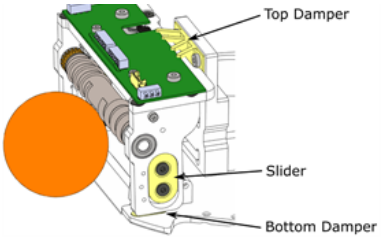

Fig. 2. CAD image for three dampers on TIGERs' robot[1].

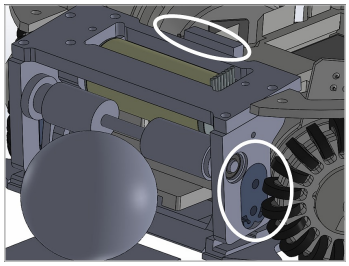

Fig. 3. Top Damper and Slider CAD image designed for our robot.

③ and ⑥ have the same shapes respectively. For sample ②, however, when the honeycomb pattern was made with the same hole diameter as sample ⑤, internal cracking occurred shortly after fabrication in the softer sample ②. Therefore, sample ② was made with larger holes and thicker surrounding lines compared with sample ⑤. Sample ① also had slightly thicker lines compared with sample ④ to enhance its strength.

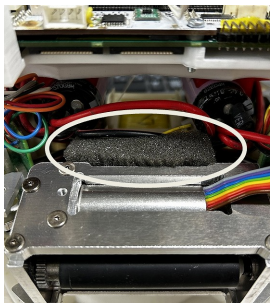

(a) Natural Rubber

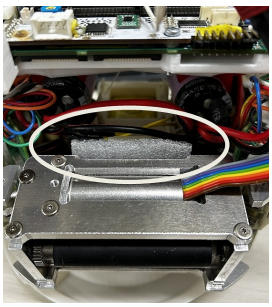

(b) Polyethylene

Fig. 4. Top Damper made from NR(Left) and Polyethylene (Right) used in the experimental.

The experimental measurement of impact absorption (damping ratio) was performed by striking a ball against a dribbler at a constant velocity, as shown in Fig.6(a), and comparing the rebounding velocity. Here, the damping ratio was defined as the difference between the incident speed and the rebounding speed divided by the incident speed. A value closer to 1 indicates a greater degree of damping. The velocity of the ball striking the dribble bar and its rebounding velocity were measured using a camera-based analysis. The obtained velocities closely agreed with the values from the speedometer. Note that we used the straight-type dribbling bar shown in Fig.6(b). This was because we predicted that the split-type used in competition would cause variance in the data de-

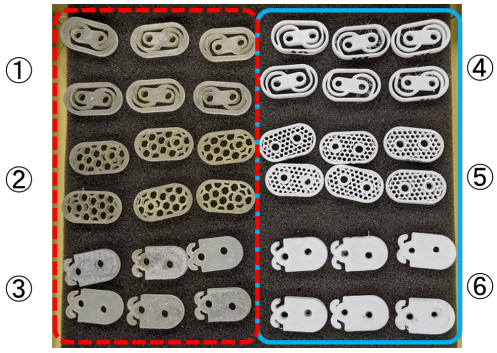

Fig. 5. Several dampers (sliders) used for the experimental, urethane-like①-③(inside of red broken-line) and TPU④-⑥ (inside of blue solid-line).

pending on the collision point of the ball. We performed 10 experiments for each damper combination and tabulated the average damping rate for ball velocity in Table 1.

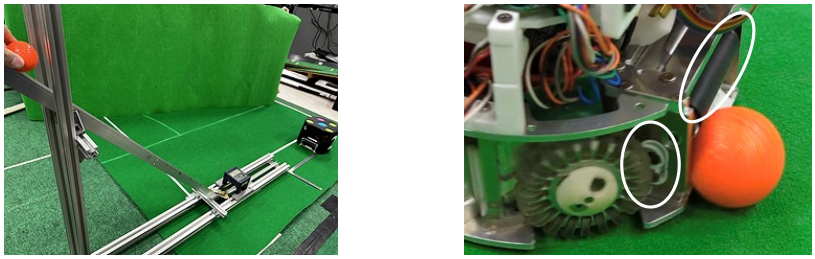

(a) Experimental condition

(b) Actual damper and straight-bar equipped on the dribble unit.

Fig. 6. Experimental method for measuring the damping rate of ball velocity.

Table 1. Damping rate of ball velocity depending on the damper combination.

Slider materials & Shapes	Silicone Rubber-like			TPU			Previous damper
	①	②	③	④	⑤	⑥	(No top damper)
Top Damper/NR(softer)	0.75	0.62	0.59	0.54	0.55	0.53	0.71
/Polyethylene (harder)	0.71	0.66	0.65	0.76	0.63	0.66	

2.3 Results and Discussions

These results indicate that the energy absorption performance (damping ratio) is better when using a softer sponge material for the Top Damper and a soft silicone rubber-like material for the Slider (e.g., NR+①). On the other hand, when a harder polyethylene sponge material was used for the Top Damper, it was found that a similarly hard TPU material for the Slider could provide equivalent or higher damping rates (e.g., Polyethylene+④). This suggests that the damping performance was enhanced by the two dampers cooperating effectively with each other. In other words, if there is a difference in the hardness of both dampers, the performance is dominated by one damper. These results suggest that the combination of the Top Damper and Slider is important for enhancing damping performance for ball velocity. Based on the above results, we participated in the RoboCup Japan Open 2025 with a combination of relatively hard polyethylene sponge and TPU④ for the top damper and slider, respectively, mounted on the robot. As the result, we achieved second place [4] next to TIGERs and confirmed improved bumper characteristics compared with previous designs for ball holding functions.

3 Analysis of Competitive Performance for SSL Team

One of the objectives in SSL is to develop tactics, but research on their effectiveness and evaluation methods is scarce. Currently, the only way to evaluate tactics is based on match results. Thus, we have been trying to evaluate using inverse analysis methods since last year[5]. In general, forward analysis generates data from a known model, while inverse analysis estimates a model from data. Most teams in the SSL League use forward analysis, creating tactical models, generating commands (data) for robots, and simulating their outcomes. On the other hand, in human soccer, inverse analysis is frequently performed to analyze the reasons or behind-the-scenes tactics based on actual match results and data. At last year's KIKS ETDP, we analyzed team performance using expected goals (xGs)[6], one of the metrics for evaluating human soccer. Similarly this year, we will analyze the game logs[7] from RoboCup 2025 to examine how the distribution of competitive performance has changed compared with last year. Furthermore, we consider methods for extending expected goals and demonstrate their potential as a new metric.

3.1 Investigation Methods and Procedures

As demonstrated in last year's ETDP[5], xGs are calculated using shooting data from ball-kicking events during matches, processed through supervised machine learning[8]. The target variable was the scoring outcome (1 for goal-scoring shots, 0 otherwise). The explanatory variables were set as: (a) the shooter's position, (b) the number of opponents between the shooter and the goal, and (c) the area where the goal could be targeted while avoiding defenders (the ratio of the width

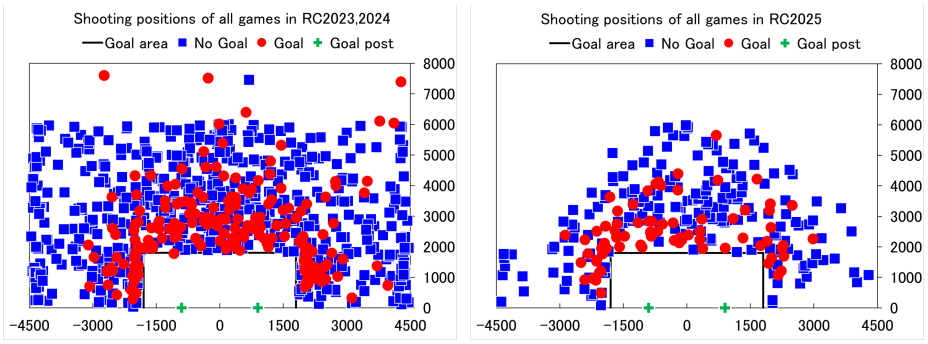

(a) 2023 and 2024 (b) 2025

Fig. 7. Sooting positions from all games in RoboCup 2023-2025 (Div-A).

of the goal that is difficult for the goalkeeper to defend relative to the total width of the goal). Using all 44 games from the 2023 and 2024 RoboCup tournaments as training data, and all 17 games from the 2025 RoboCup tournament as validation data (note: a few log files had some missing data points)[7]. An ensemble learning approach was applied to trained machine learning models (Logistic Regression, Ridge Classifier, LGBM Classifier) to derive the expected goal value. Here, the analysis program was written in Python and utilized libraries[9],[10],[11],[12]. Based on the calculated xG values, we will evaluate and analyze each team's robotic performance and the effectiveness of their tactics.

3.2 Evaluation of the Validity of the Expected Goal Model

The validity of the three models developed in this study was verified using two evaluation metrics: ROCAUC Score[13] and PRAUC Score[14]. The feature combinations for the three models, A, B and C are shown in Table 2. The bracket{} represents the explanatory variable described in Sec.3.1. These three models were trained using 820 shooting data points from RoboCup 2023 and 2024. As shown in the results in Table 2, all models are validated as effective models based on both ROCAUC and PRAUC scores. Among them, Model C achieved the best scores.

Table 2. Verification of three models by ROCAUC and PRAUC scores

	ROCAUC			PRAUC		
Characteristic feature	Logistic	Ridge	LGBM	Logistic	Ridge	LGBM
A{(a)}	0.734	0.735	0.723	0.387	0.387	0.492
B{(a),(b)}	0.769	0.768	0.749	0.428	0.428	0.538
C{(a),(b),(c)}	0.779	0.779	0.768	0.453	0.455	0.620
Random	0.5			0.234		

3.3 Expected Goals for Each Team in RoboCup 2025

Using the trained models, we calculated the expected goals (xGs) for all teams in the RoboCup 2025 tournament and compared them with the actual goals scored. We calculated the ensemble value (average prediction) for each model's xG value based on the ROCAUC scores obtained in the previous section. Note that among the RoboCup 2025 log data, two points scored by RobôCIn are lost. Additionally, one point scored by RoboDragons is excluded from the data because it was clearly an own goal. Table 2 shows the xGs and actual goals scored. The rows in each table show offensive statistics, while the columns show defensive statistics. Comparing actual goals scored with expected goals allows us to analyze the matchups between teams. First, considering offense: ZJUNlict's actual goals scored against RoboDragons were double their xGs, while against RobôCin they scored less than their xGs. For TIGERs, their total actual goals scored exceeded their xGs overall, but it was confirmed that they scored less than their xGs against some opponents. Defensively, the TIGERS allowed only one goal against opponents in the past three RoboCup tournaments. Fundamentally, due to the low number of attacking shots allowed, their xGs value is also quite low. Looking at other teams, ER-Force comes into focus. Although they placed 5th in RoboCup 2025, their defensive performance shows lower actual goals and xG values compared to higher-ranked teams like ZJUNlict and RoboDragons, suggesting they are a defense-focused team.

Table 3. Values of xGs (and actual goals) for all games in div-A RoboCup 2025

	xGs (Goals)		Defence					
	Team	Rank	TIGERs	ZJUNlict	RobôCIn	RoboDra	ER-Force	Total
Offence	TIGERs	1		22.47(15)	10.23(8)	7.40(10)	14.60(15)	54.70(48)
	ZJUNlict	2	1.37(0)		5.19(3)	4.93(10)	1.53(1)	13.02(14)
	RobôCIn	3	0.00(0)	2.05(1)		8.08(8)	1.25(0)	11.38(9)
	RoboDra	4	0.09(0)	0.00(0)	1.50(0)		3.91(0)	5.50(0)
	ER-Force	5	0.16(0)	0.67(0)	1.00(0)	6.29(1)		8.12(1)
	Total		1.62 (0)	25.19 (16)	17.92 (11)	26.70 (29)	21.29 (16)	

3.4 Development of Expected Goals Using the OBSO Model

In earlier sections, we demonstrated that expected goals can be used to analyze the validity of scoring opportunities and quantitatively evaluate the competitive performance for each team. The expected goals model, however, is based on the assumption that shooting occurs. Therefore, we are unable to evaluate the process of deciding not to shoot, i.e. the contributions made in the pre-scoring phase, such as off-ball positioning and space creation, as demonstrated by robot

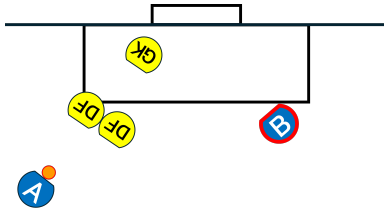

Fig. 8. A problem with evaluation based on xGs (eg. contributions of robot B) .

B in Fig.8. Thus, we try to introduce an evaluation for players without the ball and quantify scoring opportunities with a broader point of view.

According to Spearman[15], introducing the Off-Ball Scoring Opportunity (OBSO) metric allows quantifying the probability that an attacking player without ball possession will score on the next on-ball event, based on the instantaneous game state. The OBSO model aims to go beyond the limited moment of a shoot by utilizing spatiotemporal tracking data, making it possible to analyze deeper strategic features. The OBSO score is calculated as the spatial integral of the following three conditional probabilities, as following Eq.(1)[15].

$$P(G|D) = \sum_{r \in \boldsymbol{R} \times \boldsymbol{R}} P(S_r|C_r, T_r, D) \cdot P(C_r|T_r, D) \cdot P(T_r|D) \tag{1}$$

$\boldsymbol{P(S_r|C_r, T_r, D)}$ The first term in Eq.(1) represents the probability of the xG model (here, the A{a} model from Table2 is used to reduce computation time).

$\boldsymbol{P(C_r|T_r, D)}$ The second term is the Control Model, representing the probability that the attacking team can control the ball at any point on the field.

$\boldsymbol{P(T_r|D)}$ The third term is the Transition Model, predicting where the next on-ball event will occur on the field—that is, the position of the pass receiving robot.

The advantage of introducing OBSO is that it provides a quantitative evaluation of a robot that created space in a position potentially leading to a goal, even if the ball was not actually passed there. Figure 9 shows the both team's OBSO score every 1 seconds during the RoboCup 2025 final. The five red crosses marked in Fig.9 indicate the times at which TIGERs scored. The OBSO score results clearly show that the TIGERs dominated the match advantageously during most of the game. The position of the red cross exactly matches the point where the TIGERs' OBSO score dropped. This indicates that TIGERs scored while dominating the match, showing the game was restarted. This result is considered to quantitatively reflect the offensive and defensive dynamics during the

game. Therefore, by appropriately utilizing this model, it is possible to evaluate not only the quality of shooting accuracy but also a team's overall ability to create scoring opportunities from more multifaceted perspectives.

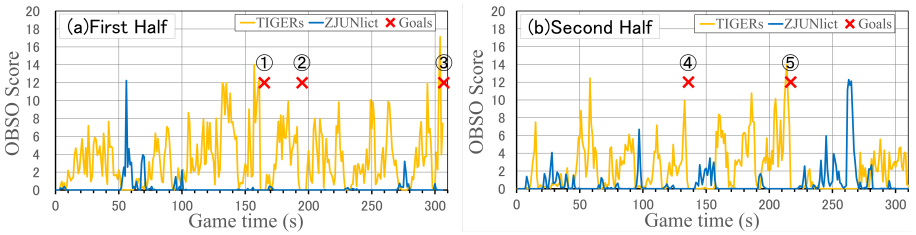

Fig. 9. Time-Dependence of OBSO Scores in RoboCup 2025 Finals. Five red crosses indicate the times at which TIGERs scored.

4 Development of an Ultra-Compact Soccer Robot Specialized for Education

We have been developing SSL robots for over 20 years. During the development activities, we have held various events in local communities and elementary schools to let children experience AI-driven control precision and the difficulty of human operation, and also to foster children's interest in science and robotics. In recent years, we have been introducing a soccer mini-game system using two actual SSL robots. One is operated by a human, while the other is controlled by AI. However, the SSL robots used in actual competitions are expensive, and repair time and costs are significant when they breakdown. We currently have no spare robots; we only have exactly the 11 robots needed for SSL competitions. Therefore, it is difficult to perform demonstrations before competitions where breakdowns are a concern, even for one-on-one matches. Furthermore, demonstrations require a relatively large field (at least 2m×3m). If sufficient space cannot be ensured, we would have had to consider modifying the demonstration method or withdrawing from the event. Thus, in this study, we try to develop a new robot that can be manufactured at low cost as an alternative to expensive soccer robots for SSL. Additionally, we aim to build an experiential system optimized for learning and educational support, making demonstrations significantly simpler. This chapter presents the specifications and configuration of the developed ultra-compact robot.

4.1 Specifications for robot

The development concept focused on constructing an economical and easy-to-build soccer robot, which was designed to fit in a palm. For the design, we decided on a production cost target of under $30 per robot by extensively using

3D printed parts and cheaper components. The robot must, nevertheless, include omnidirectional movement and kicking mechanisms as essential functions.

Structure of Omni-Directional Movement To achieve omnidirectional movement, the robot is configured with three omni-wheels arranged at angles of 120 degrees each, as shown in Fig.10(a). The 30mm-diameter omniwheel is constructed with twelve 3D-printed PLA rollers mounted along its circumference. These rollers are passed through a 1mm diameter wire and fitted into the slot on a single side of the part (Fig.10(b)). For wheel driving, a compact continuous rotation servo motor FS90R was used. The rotation speed can be adjusted via the duty ratio of the PWM signal, which simplifies the external control circuit. Although this motor has a low maximum rotation speed of 130 rpm, a 22:8 gear ratio between the motor shaft and tire shaft multiplies the rotation speed by 2.75 times.

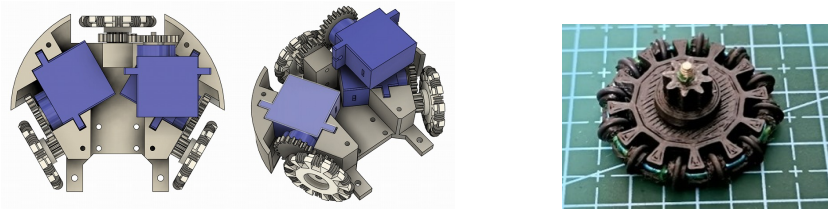

(a) Layout of motors and wheels (b) Construction of Omni-Wheel

Fig. 10. Configulation of motors and wheels.

Kicking mechanism The kicking mechanism using a spring is shown in Fig. 11(a). It consists of a combination of a SG90 servo motor and a rack gear. The mechanism works by compressing the spring and utilizing its return force to push out the ball. The spring shown in Fig. 11(b) was reused from a push-button ballpoint pen.

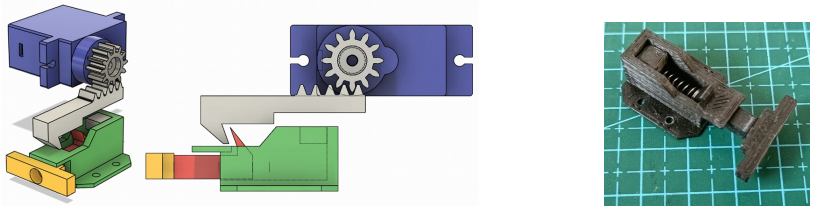

(a) Kicking mechanism (b) Spring reused from a push-button ballpoint pen

Fig. 11. Structure of Kicking Device.

Dribbling mechanism Similar to the SSL robot, the dribbler was designed with a mechanism to give backspin to the ball using rollers (Fig.12). A Tamiya Mini 4WD motor was used. Figure 13 shows the dribbler using a silicone tube with an outer diameter of 12mm. For the roller shafts, it also uses Mini 4WD ball bearings. A photoreflector was used as the ball sensor. This allows detection of whether the robot is holding the ball. This is also the same as the SSL robot.

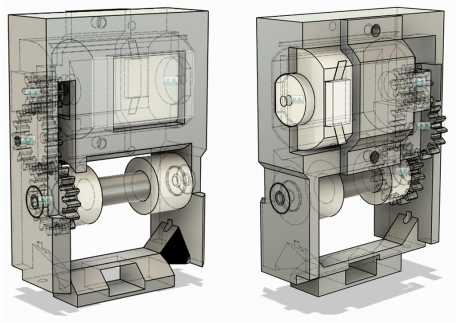

Fig. 12. 3D CAD image of Dribbling Device (Left: Front side and Right: back side)

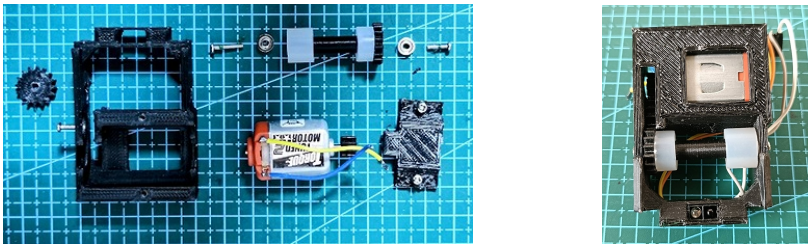

(a) Components of Dribbling Device

(b) Dribbling Device manufactured by 3D printer

Fig. 13. Structure of Dribbling Device.

Circuit Board Figure 14 shows the control circuit using the Seeed Studio XIAO ESP32C3 microcontroller. Similar to conventional SSL robots, this microcontroller includes a built-in Wi-Fi module, enabling communication with a PC via a Wi-Fi router. It also incorporates a 6-axis accelerometer MPU6050, supporting the motion control of the robot based on angular velocity. Additionally, a piezoelectric speaker for debugging allows sound confirmation of the robot's status regarding startup and communication. The power supply for the

robot uses four rechargeable AAA batteries connected in series to provide approximately 5V, matching the nominal voltage of the motors (Fig. 15(a)). The PIC microcontroller PIC16F18313 was used for controlling the dribbling motor and processing data from the ball sensor. A FET is used to drive the dribbling motor, enabling PWM control from the PIC microcontroller. For communication between the ESP and PIC, the UART is used. Threshold adjustment for the ball sensor is performed using a variable resistor on the board, and its response can be confirmed via an LED.

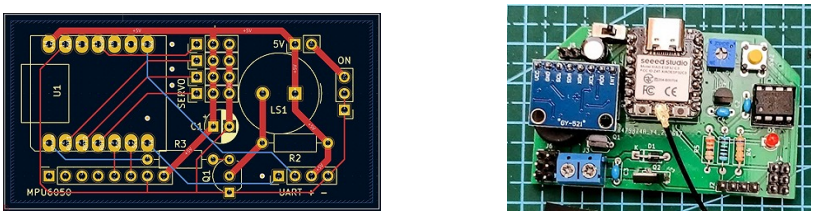

(a) Circuit pattern (b) Control circuit board

Fig. 14. Circuit pattern and actual circuit board

(a) Battery box (b) Marker equipped on a robot

Fig. 15. Battery box and hull of Robot

The hull of the robot was 3D printed with a diameter of 80 mm. To simplify battery replacement, the top of the robot was designed as an easy-to-open cover. Additionally, as shown in Fig.15, colored paper was attached from the back side. This enables autonomous operation using a camera (global vision system) set up above the field. Typical prototype robots are shown in Fig.16(a). The robot dimensions with the cover attached are 80 mm diameter, 89 mm height, and 179 g weight (227 g including battery). Figure 16(b) shows a size comparison with an SSL robot.

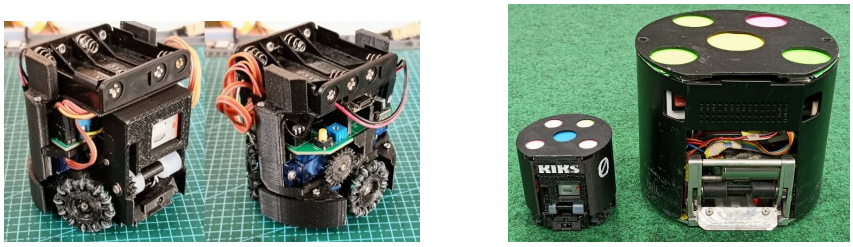

(a) Manufactured typical mini soccer robot (b) Size comparison with an SSL robot

Fig. 16. Typical soccer robot and size comparison with SSL Robot

4.2 Evaluation of Robot Performance and Applications

When moving robot straight ahead on the carpet used in RoboCup competitions, the maximum travel speed was approximately 260 mm per second. Moreover, when the robot kicked a ball from a stopped state, the initial velocity was 850 mm per second, and the distance the ball rolled was 870 mm. Here, for the measurements, a table soccer (foosball) ball, as shown in Fig.17(a) was used. With this performance, it is expected to be sufficiently usable for educational purposes and competitions. The total cost per robot was approximately $30 (one-sixtieth of an SSL robot), achieving the target amount.

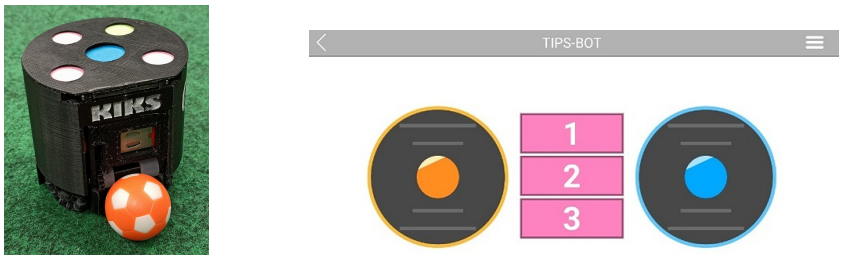

(a) Ball used for kick performance evaluation (b) RemoteXY Screen (Use the left/right sticks and center buttons to move/rotate, and perform kick actions)

Fig. 17. Ball and RemotoXY screen for smartphone applications

To operate the developed soccer robot, we introduced the free app RemoteXY(Fig.17(b)), which enables wireless robot control and can be used on smartphones or tablets. Example applications include mini soccer games using one-on-one or cooperative play with multiple robots, or matches against AI robots using conventional SSL-vision system. Regarding robot control and C programming to achieve these, there is a significant gap in skill levels among elementary and junior high school students. Therefore, we decided to provide pre-programmed basic operation programs for motor and kick-device control, and other functions.

The robot construction procedures and control program fundamentals described above, as shown in Fig.18 and Fig.19, were summarized in a text. Then, we distributed this material to educational institutions and students interested in robot development and held a lecture for teacher training students in 2025.

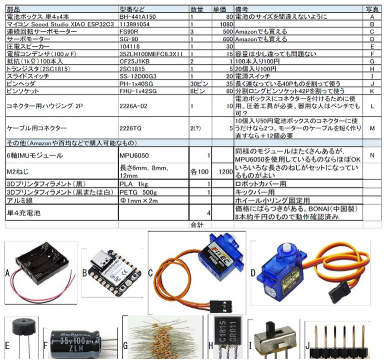

部品	型番など	数量	単価	備考	写真
電池ボックス 単4x4本	BH-441A190	1		80(電池のサイズを間違えないように)	A
マイコン Seed Studio XIAO ESP32C3	113991054	1	1080		B
連続回転サーボモーター	FS90R	3		500(Amazonでも買える	C
サーボモーター	SG-90	1		600(Amazonでも買える	D
圧電スピーカー	104118	1		30	E
電解コンデンサ:(100μF)	25ZL R100M6.3X11	1		15(容量は小し違っても問題ない	F
抵抗(1k Ω)100本入	CF25JR1KB	2		1100(本入り100円)	G
トランジスタ(2SC1815)	2SC1815	1		520(個入り100円	H
スライドスイッチ	SS-12D00G3	1		20(電源スイッチ	I
ピンヘッダ	PH-1x40SG	3(6ピン		35(長く速なっている40Pものを好って使う	J
ピンソケット	FHU-1x42SG	8(2ピン		80(分割ロングピンソケット40Pを割って使う	K
コネクター用ハウジング 2P	2226A-02	1	10	電池ボックスにコネクターを付けるために使用。圧着工具が必要。使用な人はペンチでも可	L
ケーブル用コネクター	2226TG	2(?)	5	10個入り5円電池ボックスのコネクターに使うだけなら2つ。モーターのケーブルを短く作り直すなら+12個必要	M
その他(Amazonや百均などで購入可能なもの)					
6軸IMUモジュール	MPU6050	1		同様のモジュールはたくさんあるが、MPU6050を使用しているものならほぼOK	N
M2ねじ		各100	1200	いろいろな長さのねじがセットになっているものがよい	
3Dプリンタフィラメント(黒)	PLA 1kg	1		ロボットカバー用	
3Dプリンタフィラメント(黒または白)	PETG 500g	1		キックバー用	
アルミ線	Φ1mm×2m	1		ホイールのリング固定用	
単4充電池		4		価格にばらつきがある、BONAI(中国製)は未初不円のもので動作確認済み	
		合計			

(a) Electronics and related parts list

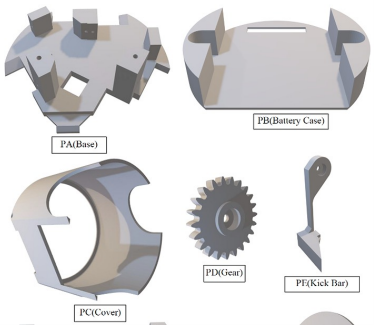

(b) 3D printed parts (STL images)

Fig. 18. An example of the contents of a textbook in Japanese (Hardware)

(a) Contents

●→プログラム 10 IMU による角速度のフィードバック制御

```
//割り込み処理
void timer1Task() {
  gyro.update();
  robo.execute(cycle);
}

//割り込み用タイマー
EspEasyTimer timer1(TIMER_GROUP_0, TIMER_0);

void setup() {
  delay(1000);
  gyro.setup();  // IMU のセットアップ
  robo.setup();  // ロボットのセットアップ
  robo.set_use_gyro(true); //ロボットの制御に IMU を使う設定にする
  Serial.begin(115200);  //シリアル通信開始
  timer1.begin(timer1Task, cycle); // 割り込み開始
}
```

(b) Feedback control using IMU

Fig. 19. An example of the contents of a textbook in Japanese (Software)

4.3 Advances in Robotics

Robots can be advanced by incorporating various sensors. A typical example is shown in Fig.20. The robot shown in Fig.20(a) equipped with an ultrasonic sensor can recognize obstacles and walls. Furthermore, the robot shown in Fig.20(b) equipped with a local camera can recognize a ball and the goals. That is, it can play the game without a global vision system (without SSL vision).

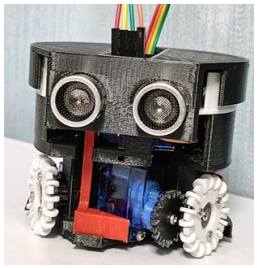

(a) With ultrasonic sensors

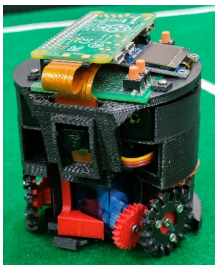

(b) With local camera

Fig. 20. Examples of advances in robot

The color recognition and control program for the camera mounted on the robot was developed in Python, using OpenCV for image analysis. The camera module in Fig.21(a) can recognize the ball up to 90 cm away from the camera when mounted at a height of 55 mm above the floor. In Fig.21(b), the orange ball and the yellow-painted goal wall are framed by white squares, which indicates they are successfully recognized.

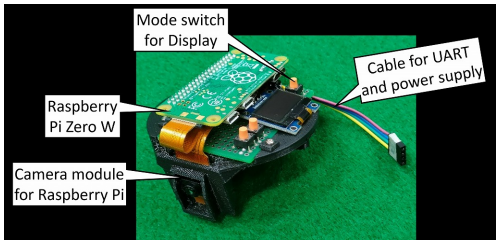

(a) Developed camera module

(b) A typical camera view

Fig. 21. Local camera module and typical view of camera mounted on robot

4.4 Operation in SSL-Vision

The robot can be run mostly without modification on the SSL system. However, for SSL-Vision, it is necessary to adjust the parameters to correspond to the robot's size. Figure 22 shows the performance verification of the developed ultra small size soccer robot. The communication between PC and the robot is the same as the method used to control conventional SSL robots. That is, it can be controlled by sending commands from the PC to the robot via the Wi-Fi system.

Acknowledgments

The authors wish to express their deep appreciation to other KIKS members for the software developments and the hardware manufacturing. This work was sup-

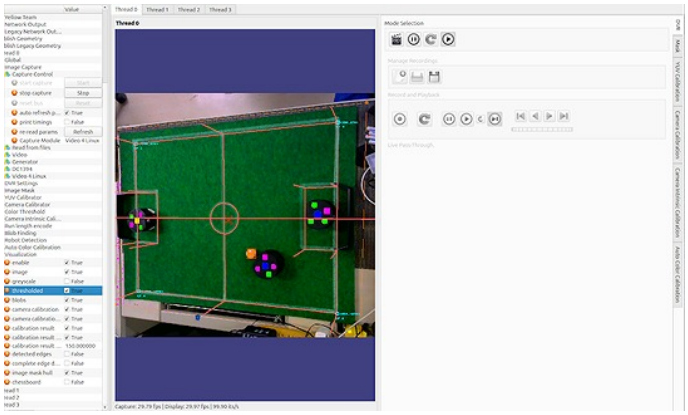

Fig. 22. Functional verification in SSL-Vision

ported in parts by Grant-in-Aid from JSPS KAKENHI Grant Number 24K06428, The Nitto Foundation and The Sango Foundation for Education in Japan, respectively.

References

1. Nicolai Ommer, Andre Ryll, Mark Geiger: TIGERs Mannheim Extended Team Description for RoboCup 2022; https://ssl.robocup.org/wp-content/uploads/2022/04/2022_ETDP_TIGERs-Mannheim.pdf.
2. Modeling Material AR-G1H (High-Hardness Silicone Rubber): https://www.keyence.co.jp/products/3d-printers/3d-printers/agilista-3100/models/ar-g1h/
3. TPU 95A 2.85mm 1000g: https://apple-tree.shop/?pid=172508249
4. Results in JapanOpen 2025: https://www.robocup.or.jp/JapanOpen2025/results.html
5. Mizuki Nonoyama et al.: KIKS Extended Team Description for RoboCup 2025; https://https://ssl.robocup.org/wp-content/uploads/2025/04/2025_ETDP_KIKS.pdff
6. Satoshi Nishikawa: Introduction to Sports Robotics Simulation·Analysis and Intervention in Competition, Ohmsha (2024) [in Japanese]
7. SSL game log: https://seafile.tigers-mannheim.de/d/e85851d9bc9944bf95bb/?p=/gamelogs/&mode=list
8. Sebastian Raschka: Python Machine Learning [in Japanese], impress top gear, 2016.
9. precision_recall: https://scikit-learn.org/stable/auto_examples/model_selection/plot_precision_recall.html
10. sklearn.linear_model: https://scikit-learn.org/stable/modules/linear_model.html
11. lightgbm: https://lightgbm.readthedocs.io/en/stable/
12. optuna: https://optuna.org/
13. roc_auc_score: https://scikit-learn.org/stable/modules/generated/sklearn.metrics.roc_auc_score.html
14. Evaluation-metrics: https://machinelearningmastery.com/tour-of-evaluation-metrics-for-imbalanced-classification/
15. W. Spearman: Beyond Expected Goals, 12th MIT Sloan Sports Analy. Conf., Boston MA, (2018).